Available online at www.sciencedirect.com
SCIENCE DIRECT®
ELSEVIER
International Journal of Solids and Structures 41 (2004) 6813–6830
INTERNATIONAL JOURNAL OF SOLIDS and STRUCTURES
www.elsevier.com/locate/ijsolstr

Evolution of plastic zones in dynamically loaded plates using different elastic–viscoplastic laws

Marcus Stoffel *

Institut für Allgemeine Mechanik, RWTH Aachen, Templergraben 64, 52056 Aachen, Germany

Received 20 April 2004; received in revised form 25 May 2004
Available online 6 July 2004

Abstract

In the framework of viscoplastic theory many different laws were developed, accounting for material behaviors like creep, relaxation or evolution of overstresses. Though each model is able to predict in uni-axial material tests the values of stresses depending on plastic strains and plastic strain rates the question is if solutions of simulations are still realistic if the viscoplastic law is applied on structural deformations. In the present study strain rate sensitive metal plates are subjected to shock waves. The purpose is to compare simulation results obtained with different elastic–viscoplastic laws to experiments in order to determine the most appropriate material model. By subjecting circular metal plates experimentally to shock wave loadings realistic deformation histories are measured. The measurements are compared to simulation results obtained with different viscoplastic laws. The aim is to find out the accuracy of each model concerning the predictions of displacements, shape formings, spread of plastic zones and evolutions of inner bending moments.

Keywords: Dynamics; Shock waves; Elastic–viscoplastic; Mechanical testing

1. Introduction

In viscoplastic theories the deformation velocity plays an important role in predicting plastic deformations. Basic knowledge for calculating the strain rate dependence between stresses and strains was introduced by Andrade and Da (1910) in the case of creep. Three different stages of this viscoplastic phenomenon were described: primary creep where the hardening is dominant leading to a decreasing strain rate. During the secondary creep the material develops plastic strains with constant strain rate and in the case of tertiary creep the strain rate increases and material damage can occur. Norton (1929) proposed for secondary creep a law with two viscous material parameters in order to describe the relationship between stress and plastic strain rate. This law is of elementary importance for calculating overstresses depending on

* Tel.: +49-241-8094601; fax: +49-241-8092231.
E-mail address: stoffel@iam.rwth-aachen.de (M. Stoffel).

0020-7683/$ - see front matter © 2004 Elsevier Ltd. All rights reserved.
doi:10.1016/j.ijsolstr.2004.05.060

the deformation velocity which is used in many viscoplastic laws. This phenomenological description of the overstress holds not only in creep processes but also in high dynamical deformations. Therefore, the propagation of plastic waves in rods during impact tests were predicted by Malvern (1951) with viscoplastic constitutive equations using the overstress versus strain rate relation proposed by Norton (1929). In the contrary attempts by Taylor (1940) and von Kármán (1942) describing wave propagations with strain rate independent constitutive laws lead to differences between measured and calculated strains. The reason therefore was the missing overstress in the material model. Three-dimensional viscoplastic constitutive equations were introduced by Perzyna (1963) assuming perfect plastic material behavior. Chaboche (1989) and Lemaitre and Chaboche (1994) developed similar laws accounting for non-linear hardening. Following this method of using overstresses in three-dimensional continuum mechanics several authors proposed their own viscoplastic models, e.g. Tanimura (1979), Krempl et al. (1984), Krempl and Khan (2003), Lehmann (1984), Bruhns (1987), Imatani et al. (1991), Uenishi and Teodosiu (2004) or Colak (2004). Gurtin (2003) presented a viscoplastic theory based on a system of microforces and derivated a weak formulation of a non-local flow rule. Rizzi and Hähner (2004) derivated a model to describe plastic material instabilities and found an agreement to experimental observations. In order to cover in the constitutive equations also rate dependent elasticity Lubarda et al. (2003) extended an overstress model to a general viscoelastic–viscoplastic law. The essential characteristic of the mentioned viscoplastic laws is that a yield limit depending on the strain rate is used, separating elastic and inelastic material behavior from each other. In contrast to classical plastic flow rules using the second stress invariant, Iyer and Lissenden (2003) used all three stress invariants in the threshold function and applied this model to alloy at high temperatures. The problem of rate dependent damage was also covered in the framework of a viscoplastic theory presented by Voyiadjis et al. (2004). Furthermore, viscoplastic laws were developed which do not distinguish between elastic and plastic strains. For example Bodner and Partom (1975) and Walker (1981) proposed constitutive equations assuming that every stress state behaves viscoplastic.

Also extensions of rate dependent material behavior for the case of finite viscoplasticity were carried out, e.g. by Lin and Brocks (2004) who developed a finite strain viscoplastic law using a new dissipation inequality and presented a numerical algorithm. Schneidler and Wright (2003) applied finite viscoplastic deformations also to arbitrarily anisotropic materials. Other anisotropic constitutive equations were e.g. proposed by Haupt and Kersten (2003), Tsakmakis (2004), and Häusler et al. (2004).

In the present work isotropic constitutive equations for small plastic strains are chosen from two classes of viscoplastic models, with and without yield limit. The magnitude of strains in the presented calculations is not greater than 5%. But the strain rates in the shock wave loaded structures can increase up to $200\frac{1}{s}$. Within these ranges of strains and strain rates the chosen constitutive models can be applied without leaving their domain of validity. The three-dimensional time dependent constitutive equations lead to complex mathematical descriptions especially if non-linear hardening is considered. Therefore the question arises if the viscoplastic model is overloaded and if some parts of the material behavior (e.g. hardening) can be neglected in order to save computer capacity. The effect of time consuming calculations is additionally intensified if calculations of structural responses are concerned, leading to geometrical non-linearities.

Therefore the aim is not only to determine which models are able to predict the deformations, plastic zones and the evolutions of bending moments accurately, but also to find out which parts of the viscoplastic law can be neglected, leading, however, to sufficient good correlations to the measurements.

In order to obtain calculation results of deformed viscoplastic plates, which can be compared to measured deformations, the viscoplastic constitutive equations are combined with a first-order shear deformation shell theory described in Section 3. Implemented in a finite element code simulations can be carried out and are compared to measurements. Here the following viscoplastic laws are applied:

First, the model of Chaboche (1989), consisting of three essential parts: the elastic domain, the hardening part and the viscous behavior, i.e. the part of the model being responsible for the development of

overstresses. In order to determine which part of the elastic–viscoplastic model is responsible for a proper prediction of the observed deformations or which parts could be neglected the material model is reduced to a more simple description. For example it could make sense to neglect the elastic part if the plastic strains are dominant or the hardening could be neglected, if the plastic strains are very small. Here two assumptions connected with the Chaboche model are introduced, elastic–perfectly plastic and rigid–perfectly plastic material behavior, but the strain rate sensitivity is still considered. The consequences of these simplifications will be traced beginning with the evolution of bending moments and shape forming until to the final deformation of the plate.

Second, the Tanimura model (1979) is chosen because this law was introduced by its author as a constitutive model being suitable for deformation processes with high strain rates. It uses also a yield limit but assumes perfect plasticity.

Third, in order to apply a model which does not use a yield limit the Bodner–Partom law (1975) is also taken into consideration. In this constitutive model it is not possible to separate elastic and inelastic material behavior from each other because every stress state is assumed to be viscoplastic.

In order to simulate the deformations of impulsively loaded metal plates a structural theory is applied, which can be connected in a finite element code with each of the examined viscoplastic models separately. The results of the simulations can be compared to measured deflections.

In literature a wide range of comparative studies can be found. Here only those articles are discussed which consider both, calculated and measured structural deformations. Several approaches are reported on how to investigate the inelastic dynamic behavior of structures subjected to impulsive loading experimentally and to simulate the response numerically based on various constitutive models and structural theories. An overview of relevant articles in this field is given e.g. by Cristescu (1967), Jones (1989) and Stronge and Yu (1993). In several studies explosions were used to subject structures to impulsive loadings (Idczak et al., 1981; Renard and Pennetier, 1996) and the final deformations were measured. In the present paper shock tubes with sensors for recording the pressure and the middle point displacement of the plates during the time are used. The advantage of the shock tube technique is the evolution of plane shock wave fronts (Gerard, 1956), thus yielding a uniformly distributed pressure pulse on plate specimens. This allows a measurement of the pressure impulse by sensors, which are integrated in a ring flange next to the plate. In the contrary spherical shock wave fronts generated by detonations lead to a complex pressure distribution on the examined structure.

In order to calculate the deformations observed in experiments many combinations of structural and constitutive models have been applied. Florence (1966) considered rigid–plastic material behavior applied to impulsively loaded plates. The experiments were performed with sheet explosives; final deformations were measured and compared to numerical simulations. Bad correlations were explained by an insufficient plate theory not taking membrane forces into account. Wierzbicki and Florence (1970) modified the constitutive model by using a viscoplastic law for large displacements. Their study showed that strain rate sensitivity and membrane forces have equally important strengthening effects. Kłosowski et al. (1995) applied models of Chaboche (1989) and Bodner and Partom (1975) and made comparative studies of structures under various types of impulsive loads and obtained different results depending on the used model. However, the material parameters for the respective models were taken from different sources in the literature. Kalthoff and Winkler (1987) and Kalthoff (2000) observed experimentally for impact loaded prenotched steel plates a dependency between impact speed and the kind of failure mode, brittle or ductile. Batra et al. (2003) studied this effect numerically and was able to describe this effect by applying the Bodner–Partom law (1975). Also in impact experiments, where much higher strain rates can occur than in the present study, good correlations between measurements and calculations were obtained. For example a constitutive-microdamage model was introduced by Eftis et al. (2003) in order to simulate shock compressions and fractures caused by hypervelocity impacts. Calculated results were compared to experiments in order to show the capability of the model. In a combined numerical/experimental study of

Kajberg et al. (2004) about tension tests at high strain rate (over 10^4 s^{-1}) with steel specimens the deformations are measured by digital photographs. By comparing measurements to finite element calculations material parameters are identified.

In the present work the simulations are carried out by non-linear transient finite element analysis. The determination of the material parameters with uni-axial tension tests is described by Stoffel et al. (2001b) in detail.

The measurements presented in this study are obtained by using two shock tubes subjecting circular metal plates to impulsive loadings. The pressure acting on the plate is measured by piezoelectric sensors and the plate deflection is recorded by a capacitor, developed for fast changes of displacements. This way not only final deformations are measured but also the plate deflection during the impulse duration. This technique was first used in works of Stoffel et al. (1998) and extended by Weichert and Stoffel (1998) and Stoffel et al. (2001a,b).

2. Viscoplastic constitutive equations

2.1. Chaboche model

The constitutive equations of the Chaboche model are applied in the following form:

$$\dot{\varepsilon}_{ij}^{p} = \frac{3}{2}\dot{p}\frac{s'_{ij} - X'_{ij}}{J_2(s'_{rs} - X'_{rs})}, \tag{1}$$

$$\dot{p} = \left\langle \frac{J_2(s'_{ij} - X'_{ij}) - R - k}{K} \right\rangle^{n}, \tag{2}$$

$$\dot{X}_{ij} = \tfrac{2}{3}a\dot{\varepsilon}_{ij}^{p} - sX_{ij}\dot{p}; \qquad \dot{R} = b_1(b_2 - R)\dot{p} \tag{3}$$

with the abbreviations ε_{ij}^{p}, p, s_{ij}, X_{ij}, R, $()'$, $J_2()$ denoting Green–Lagrange plastic strain tensor, equivalent plastic strain, second Piola–Kirchhoff stress tensor, backstress tensor, isotropic hardening, the deviatoric part of a tensor and equivalent von Mises stress, respectively. The yield limit k and the material parameters a, s, b_1, b_2, n, K must be obtained from tension tests. These tests were performed with specimens cut from the same metal sheets as the plates used in the shock tube experiments (see Section 4). Since only tension tests could be performed with 2 mm thick specimens, a separation of isotropic and kinematic hardening was not possible. Therefore in the Chaboche model pure kinematic hardening is assumed. With this kind of hardening a good convergence in the simulations in former studies was observed.

In order to reduce the elastic–viscoplastic law to the elastic–perfectly plastic material behavior the hardening parameters are set equal to 0. As far as rigid–perfectly plastic material properties are concerned it is in the finite element program, used in the present study, not possible to neglect the elastic material behavior, because the stresses are calculated by the elastic part of the total strains. Therefore the Young's modulus is set to a very high value.

2.2. Tanimura model

The Tanimura model is expressed by the following equations:

$$\dot{\varepsilon}_{ij}^{p} = \frac{3}{2}r\dot{p}\frac{s_{ij}}{J_2(s_{ij})}, \tag{4}$$

$$\dot{p} = \mathrm{e}^{\frac{-S_0}{\frac{1}{\sqrt{3}}J_2(s_{ij}) - \tau^*}} \tag{5}$$

with the material parameters S_0, r, τ^*, which have to be determined from uni-axial tension tests. The simplifications used for the Chaboche model are not carried out with the Tanimura model again, because both models have similar structures. This additional overstress model is applied here because it was introduced by Tanimura (1979) especially for high dynamical deformation processes and derivated for the sake of simplicity without hardening.

2.3. Bodner–Partom model

In order to use alternatively a law, which does not separate between elastic and plastic material behavior the Bodner–Partom model (Bodner and Partom, 1975) is applied in this study expressed by the following equations:

$$\dot{\varepsilon}_{ij}^{p} = \frac{3}{2}\dot{p}\frac{s'_{ij}}{J_2(s'_{rs})}, \tag{6}$$

$$\dot{p} = \frac{2}{\sqrt{3}}D_0\mathrm{e}^{-\frac{1}{2}\left(\frac{R+D}{J_2(s'_{rs})}\right)^{2n}\frac{n+1}{n}}, \tag{7}$$

$$D = X_{ij}\frac{s_{ij}}{J_2(s_{rs})}, \tag{8}$$

$$\dot{R} = m_1(R_1 - R)\dot{W}_{\mathrm{p}}, \tag{9}$$

$$\dot{W}_{\mathrm{p}} = s_{ij}\dot{\varepsilon}_{ij}^{p}, \tag{10}$$

$$\dot{X}_{ij} = m_2\left(\frac{3}{2}D_1\frac{s_{ij}}{J_2(s_{rs})} - X_{ij}\right)\dot{W}_{\mathrm{p}}. \tag{11}$$

Here W_{p} denotes the plastic work and the material parameters n, D_0, D_1, R_1, m_1, m_2 have to be identified from tension tests. For the identification of the material parameters a method proposed by Chan et al. (1988) is used.

3. Plate theory and numerical approach

In order to calculate the plate deformations in the geometrically non-linear range, observed in the experiments, a shell theory is used, assuming small strains and moderate rotations. In former studies (Stoffel et al., 2001b) it was proved that this theory is suitable for the considered magnitude of strains and displacements. The derivation of this shell model was presented by Schmidt and Reddy (1988) and Schmidt and Weichert (1989) in detail and is applied in this study for plates. By using a first-order shear deformation hypothesis expressed by the components of the displacement vector in the plate space in the form

$$v_\alpha = \overset{0}{v}_\alpha + \theta\overset{1}{v}_\alpha; \qquad v_3 = \overset{0}{v}_3; \quad \alpha = 1,2, \tag{12}$$

also shear deformations are taken into account and thickness changes are neglected. Here $\overset{0}{v}_\alpha$, $\overset{0}{v}_3$ denote the displacement components, $\overset{1}{v}_\alpha$ are the rotations at the midsurface, and θ is the normal coordinate. In order to

trace the evolution of each material parameter in the plate space the structure is divided into layers (Kreja et al., 1997). For the numerical solution of this model a finite element program is used, developed by Palmerio et al. (1990) and extended in works of Kreja et al. (1997), Kłosowski et al. (1995), and Stoffel et al. (2001b).

4. Experimental set-up

For the experiments two shock tubes are used. In tube A (Fig. 1) circular steel and copper plates with diameters of 138 mm are subjected to impulsive loadings and in tube B (Fig. 2), the greater shock tube, aluminium plates with 553 mm diameter are used. All plates are 2 mm thick and are clamped between two ring flanges. Each shock tube consists of a high pressure chamber (HPC) and a low pressure chamber (LPC), separated from each other by a membrane. By increasing the pressure in the HPC up to a certain value the membrane breaks and a shock wave is traveling through the LPC, striking the plate at the end and leading to a high-pressure and high-density impulse. During the impulse duration the history of the pressure on the plate is measured by piezoelectric sensors suitable to record fast changes of pressure. They are located in front of the plate in a separate ring flange. In order to measure the middle point displacement of the plate a capacitor is used, one plate of the capacitor is the circular front plate of the measuring device and the other one is the plate specimen. The vibration of the plate specimen results in a change of the voltage applied to the capacitor. A calibration curve relating the measured voltage and the distance between the capacitor plates to each other has to be determined before the experiment starts. The temperature dependence of the capacitor requires the calibration before each new experiment.

Depending on the gas used in the HPC and on the length of the HPC different evolutions of the pressure history can be generated; details about these fluid dynamic effects are described by Stoffel (2000). In order to

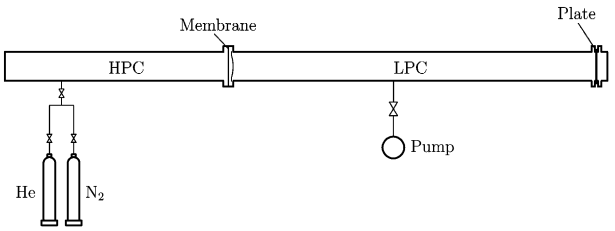

Fig. 1. Principle of shock tube A.

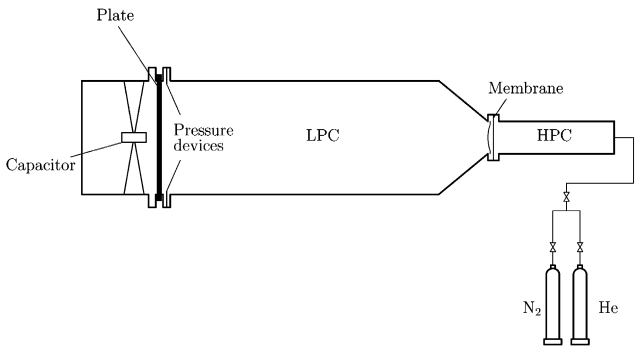

Fig. 2. Principle of shock tube B.

adjust the short impulsive loading the HPC is filled with helium, because the lighter the gas, the faster the shock wave. This causes a very fast shock wave with a short impulse duration. Furthermore, the shock period can be decreased by shortening the HPC. The reason for this is as follows: when the membrane breaks a shock wave moves into the LPC, besides an expansion wave is generated traveling first into the HPC. It is reflected at its end and reaches finally the plate specimen, thus, destroying the high-pressure state due to the shock wave. Here the HPC of shock tube A has a length of 5 m, the HPC of tube B 1 m. The entire lengths of tubes A and B are 12 m and 8 m, respectively. Two shock tubes for the experiments with different plate materials and with the described possibilities to modify the loading history are used in order to verify that the measured results are not caused by accident for one special geometry or material but also hold in a more general case. All pressure evolutions shown in this study in Figs. 3, 11, 17, and 18 are generated with helium in the HPC of the respective shock tube.

5. Comparison between experiment and simulation

First the characteristic properties concerning the propagation of bending moments in shock wave loaded plates and their influence on the evolution of plastic zones are studied. Then simplifications using the Chaboche model are introduced and other viscoplastic laws are applied. As long as overstress models are used the elastic material behavior is described by Hooke's law. The determination of the boundary conditions and the damping are described in detail by Stoffel (2000) and Stoffel et al. (2001b). In the legends of Figs. 3, 11, 17, and 18 it is denoted in brackets with (Sim.) and (Exp.) if the results are obtained by simulations or experiments, respectively. For the loading histories in the simulations the measured pressures shown in the diagrams are used.

5.1. Propagation of bending moments and spread of plastic zones

In this chapter it is shown that the spread of plastic zones is dominated in the first millisecond after the plate is loaded by a shock wave. During this time the bending moments and inner forces propagate the plate leading to plastifications which have significant influence on the final shape of the deformed plate. In the following a comparison between measured and simulated plate deformations using the Chaboche model without simplifications is presented.

In Fig. 3 a measured plate deflection obtained with shock tube B together with a simulated middle point displacement versus the time is plotted and a good correlation between simulation and experiment can be observed. In each experiment the surface at the bottom of the plate is loaded by the shock wave. The evolution of the simulated normal stresses in radial direction in the plate can be traced in Fig. 4 where they are presented at the bottom of the plate with respect to the time immediately after the shock wave loading. While the stress at the boundary is increasing monotonically the stress evolution in the midpoint shows an oscillating behavior. According to Doyle (1997) it is known that impulsively loaded structures are propagated by flexural waves leading to a wide frequency spectrum with different amplitudes. Furthermore the propagation velocity of flexural waves increases with their frequency. A spectral analysis of the present oscillation of the bending moment indicates that the highest amplitudes belong to the smallest frequencies. Due to the entire loading of the plate by a plane shock wave front the flexural wave propagation starts at the boundary. This results in the oscillating behavior of the normal stress in the midpoint shown in Fig. 4. The wave parts with the highest frequencies, highest propagation speed and lowest amplitudes reach the midpoint first, followed by parts with slower propagation speed and higher amplitudes. At the plate boundary an oscillation does not occur because there the wave propagation has its origin. If this stress behavior is summarized through the entire cross section area the resulting bending moment in the respective points can be calculated. This result is presented in Fig. 5. At the plate boundary again a monotonic

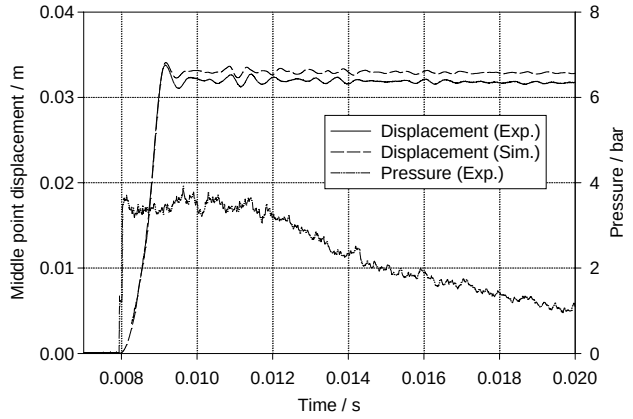

Fig. 3. Viscoplastic vibrations (shock tube B).

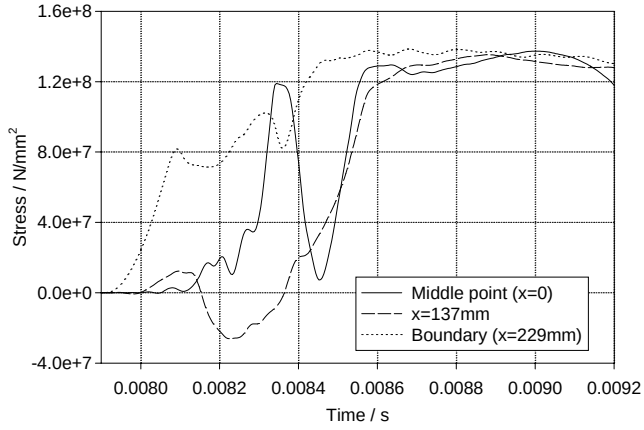

Fig. 4. Evolution of stresses at the bottom of the plate.

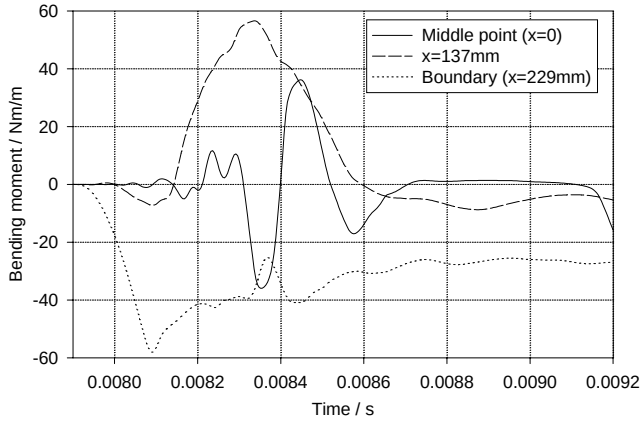

Fig. 5. Radial bending moments.

increase can be observed while in the midpoint the oscillation occurs again. The bending moment becomes 0, developing a membrane state, if the middle point displacement in Fig. 3 reaches its first amplitude. The bending moment in Fig. 5 is shown in radial direction. A positive value causes positive stresses in the top of the plate. It should be remarked that in the framework of bending theories of plates only positive bending moments should develop, leading to negative stresses at the bottom. However, positive stresses are also generated due to the oscillating bending moment. Together with the normal force (see Fig. 6) and the shear forces which are very small and not shown here, plastic strains in the plate center can develop. Because of the symmetry the normal force and the bending moment are acting from two directions rectangular to each other in the plate midsurface. The equivalent plastic strain rate is shown in Fig. 7 for three different points at the bottom of the plate. By comparing Figs. 5 and 7 the influence of the oscillating bending moment in the midpoint can be regarded. In Fig. 7 the shock wave loading starts at 0.0079 s and between 0.0083 and 0.0084 s on the time scale a plastification occurs. During this time the bending moment is negative causing positive stresses at the bottom of the plate. That means positive stresses caused by the bending moment and by the normal force are superposed. This development of plastic zones by superposition of positive stresses

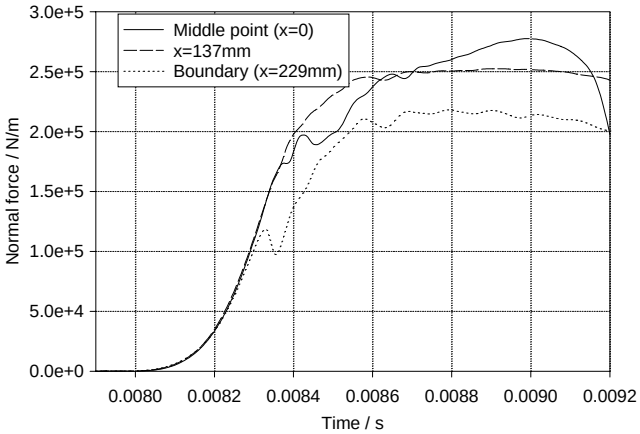

Fig. 6. Normal forces.

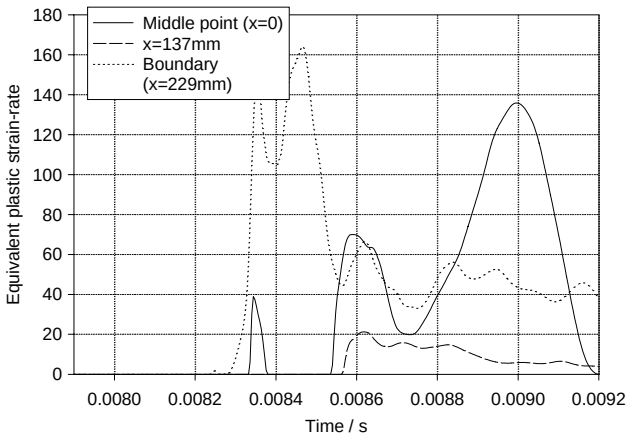

Fig. 7. Equivalent plastic strains at the bottom of the plate.

at the bottom is only possible if the oscillating character of the bending moment is predicted in the simulation. Otherwise in bending theories of plates which do not take the propagation of bending moments immediately after the pressure loading into account only negative stresses due to bending at the bottom of the plate are possible diminishing the positive stresses of the normal forces.

Immediately after 0.0084 s the plastification at the bottom in the midpoint vanishes due to an unloading of the bending moment. Because now the positive bending moment causes negative stresses at the bottom and consequently reduces positive stresses caused by the normal force. After 0.0085 s the bending moment changes again its direction causing further plastic strains at the bottom in the midpoint.

After the bending moment (Fig. 5) becomes 0 a membrane state is developed and the normal forces in Fig. 6 becomes dominant causing further plastic strains in Fig. 7. After the first amplitude of the plate deflection (Fig. 3) is reached and the movement of the middle point displacement changes its direction the plate is unloaded and after repeated oscillations only small further plastifications occur. The time scale in Figs. 4–7 represents the period of the first amplitude of the deflection in Fig. 3.

In Fig. 8, where the half of the plate is shown at several times after the plate was loaded by the shock wave, the influence of the oscillating bending moment on the shape of the deformed plate is studied. While the bending moment at the plate boundary increases monotonically after the shock wave has loaded the plate, the plate center in Fig. 8 is slightly vibrating due to the oscillating bending moment. The curvature in the midpoint is changing analogously to the direction of the bending moment. This results in a trapezoidal shape of the deformed plate in Fig. 8. After the membrane state has occurred a conical shape of the deformed plate is caused (Fig. 9). For comparison in Fig. 10 the difference between final shapes of impulsively and quasi-statically deformed plates are shown. Here a plate was subjected to an impulsive loading with 3.5 bar and another plate was loaded quasi-statically with the same peak pressure. In order to compare the shapes of plates deformed with different loading velocities a third plate was loaded quasi-statically as long as the center deflection was equal to the middle point displacement of the dynamically deformed plate. The result is a spherical form of a quasi-statically deformed plate in contrast to the conical shape of the shock wave loaded plate.

Because of the good agreement between measured and calculated plate deflections the elastic–viscoplastic material law used in this chapter is assumed to be suitable to predict the realistic dynamic plate response. Consequently the calculated propagation of bending moments, being responsible for plastic yielding in the shown simulation results, have to be predicted also by calculations using other material laws. Otherwise the calculated results could not lead to proper correlations to the experiments.

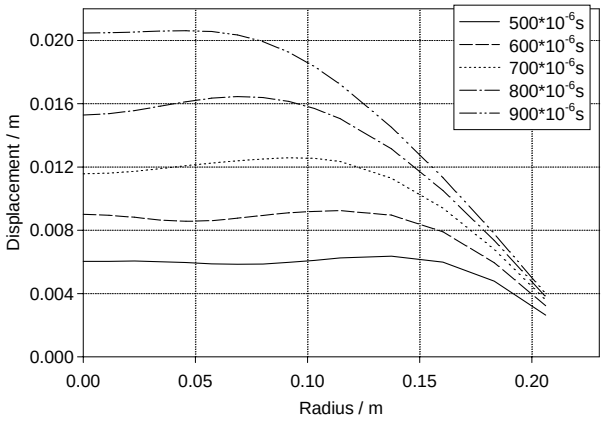

Fig. 8. Trapezoidal shape of the plate.

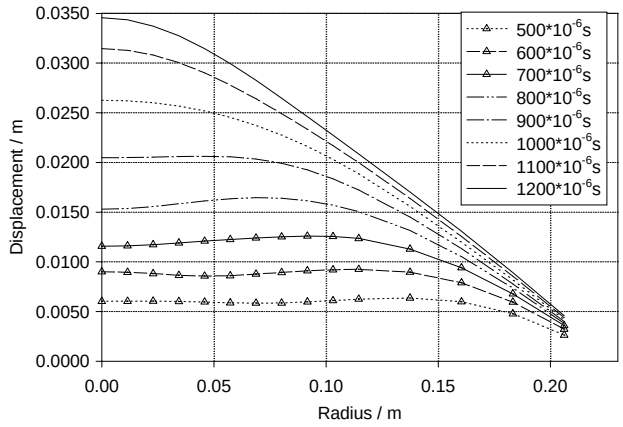

Fig. 9. Conical shape of the plate.

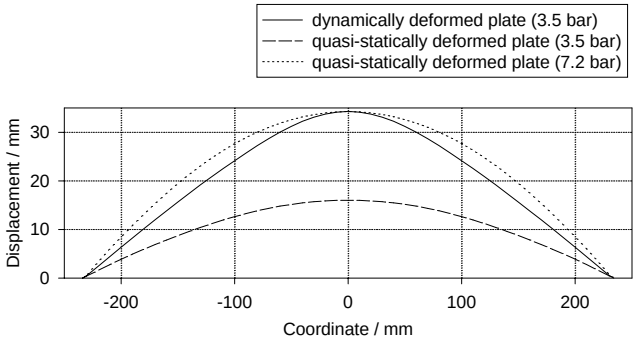

Fig. 10. Comparison between dynamically and quasi-statically deformed plates.

The study in this chapter showed the significant influence of the propagation of bending moments on the spread of plastic zones in the plate and on the shape forming of the plate. In the first millisecond after the plate was loaded by the shock wave the oscillation of the radial bending moment controlled the plastification. Therefore it is necessary to use in the following material models which are able to predict the essential propagation of bending moments.

5.2. Simulations using the Chaboche model with simplifications

After the propagation of the generalized forces in the plate and the development of plastic zones was calculated in Section 5.1 for the general elastic–viscoplastic law, it is now discussed how the non-linear elastic–viscoplastic model can be reduced to a more simple description without leading to unrealistic simulation results. Furthermore it is investigated how important the consideration of elastic material behavior is for the evolution of plastic zones in the plate. By comparing the calculated results to experiments and to simulations using the elastic–viscoplastic model of Section 5.1 the most accurate simulation is determined.

In Fig. 11 measured and simulated plate deflections versus the time are shown. The experiments are carried out with circular steel plates in tube A (Fig. 1) and in all simulations strain rate sensitivity is

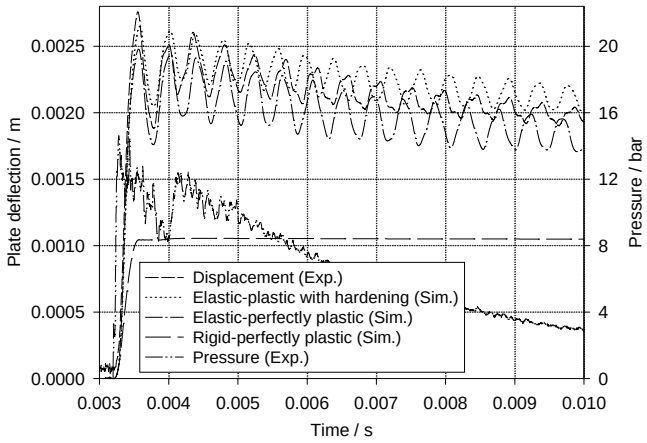

Fig. 11. Viscoplastic vibrations (shock tube A).

considered. The three simulations are carried out using elastic–viscoplastic, elastic–perfectly plastic and rigid–perfectly plastic material properties, respectively. As long as the elasticity of the material is taken into account a good agreement between simulated and measured deformations is observed but if the elastic part is neglected the simulation leads to inaccurate results. In order to study the evolution of bending moments and plastic zones in the plate more detailed, in Fig. 12 the radial bending moments in the plate center are shown versus the time for all three kinds of material laws. In the case of elastic–plastic material behavior an oscillation of the bending moment can be observed, which does not occur if rigid–perfectly plastic material properties are assumed. In order to ensure if the wave propagation vanishes due to the missing elastic part, in Fig. 13 the evolution of the bending moment of Fig. 12 in the case of elastic–plastic behavior with hardening is shown using different Young's moduli. Starting with the original elastic property ($E = 198.6 \times 10^9$ N/mm^2) an oscillating behavior is visible but with an increasing Young's modulus towards infinite this effect vanishes. After a time period T the first lower amplitude of the oscillating bending moment is reached. Using higher Young's moduli a shifting of the amplitude with time t_1 is observed which can be taken as a measurement for the vanishing oscillation. That means for the calculation of propagating

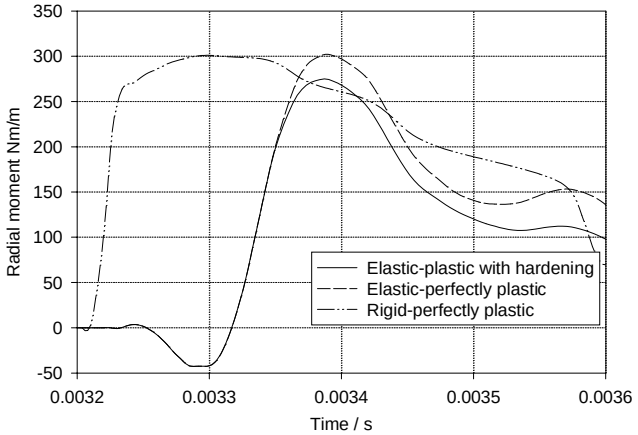

Fig. 12. Evolution of bending moments.

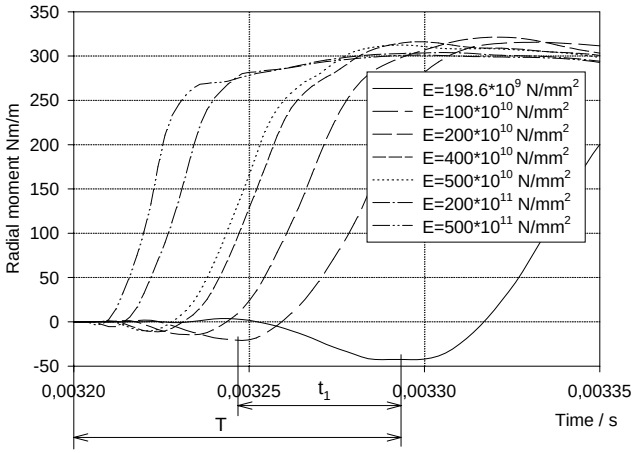

Fig. 13. Bending moments with different Young's moduli.

bending moments it is important to include the elastic material behavior. The hardening property appears not to play an important role because even the simulation in Fig. 11, which does not take the hardening into account, leads only to a small variation in comparison to the calculation with non-linear hardening.

In order to study the influence of assumptions in the material law of another generalized force in Fig. 14 the circumferential bending moment at the boundary is presented for all three kinds of constitutive equations. Here also a big deviation in the development of the moment is visible, if the elastic material behavior is neglected. The entire distribution of the circumferential moment over the plate radius at several times is presented in Fig. 15. Here also rigid–perfectly plastic as well as elastic–perfectly plastic material properties are assumed. It can be observed that in the case of rigid–perfectly plastic material behavior the circumferential moment is nearly constant over the plate surface and changes in time. In the contrary an oscillating character occurs as long as elastic material properties are taken into account.

The different evolutions of the bending moments have significant influence on the development of plastic zones in the plate (see Fig. 16). Here the equivalent plastic strain rate is shown in the top of the plate center. The magnitude of plastification is much smaller if a rigid–perfectly plastic material law is used than in the

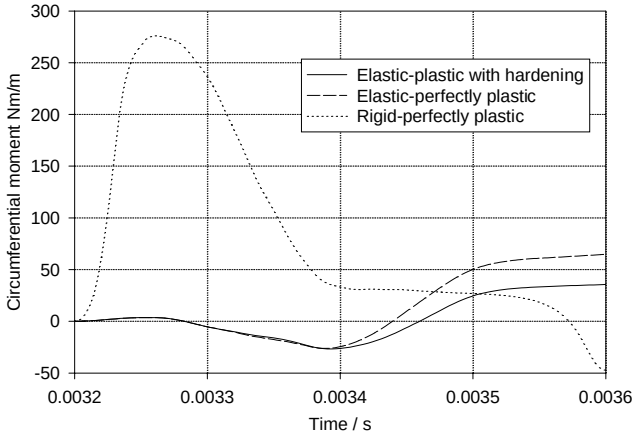

Fig. 14. Evolutions of circumferential moments.

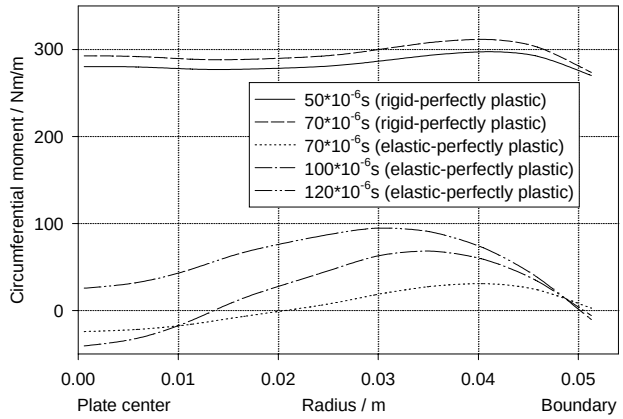

Fig. 15. Distributions of circumferential moments over the plate radius.

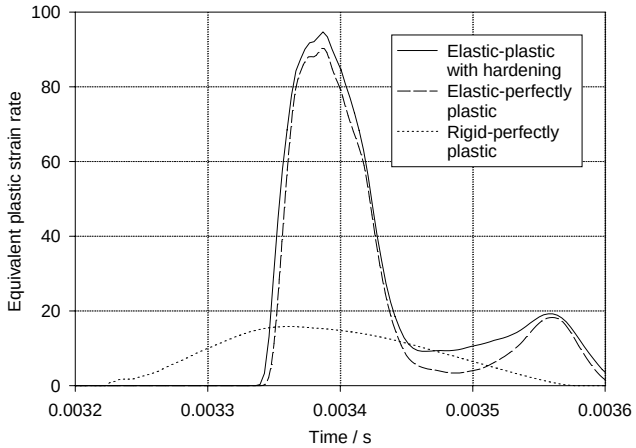

Fig. 16. Equivalent plastic strains in the top of the plate center.

case of elastic–plastic material behavior. This observation is in agreement with the small deflection in the case of rigid–perfect plasticity in Fig. 11. In Fig. 17 inelastic measured and simulated vibrations of aluminium plates with a diameter of 553 mm are shown. In this case the simulation using the rigid–perfectly plastic model including strain rate sensitivity leads to a better correlation with the experiment than the one in Fig. 11. This is due to the fact that the plastic strains compared with the total strains for the plate deformations in Fig. 16 are greater than in the case of the deformations in Fig. 11.

It can be summarized that also a good correlation to the experiment can be observed if hardening effects are neglected. But it is necessary to include the elastic material properties in order to predict the evolutions of oscillating bending moments which are responsible for the plastification.

5.3. Simulations using the Chaboche, Tanimura and Bodner–Partom models

In Figs. 17 and 18 simulated and measured middle point displacements are shown using shock tubes B and A, respectively. In both diagrams the simulations using the overstress models show the best correla-

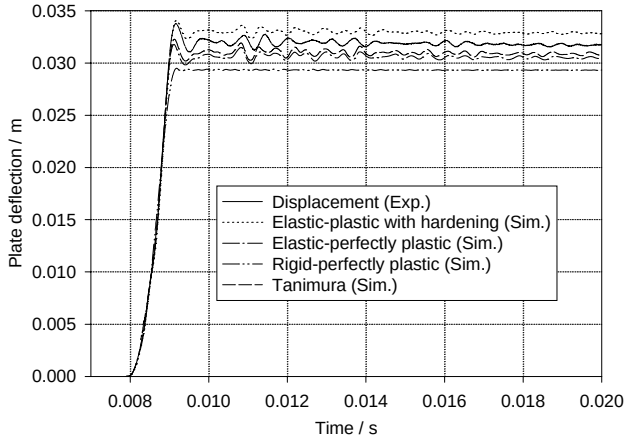

Fig. 17. Viscoplastic vibrations (shock tube B).

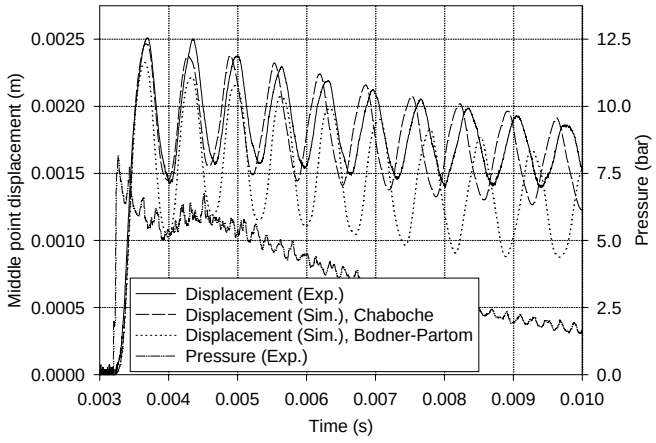

Fig. 18. Viscoplastic vibrations (shock tube A copper).

tions to the experiments. In Fig. 17 the first three simulations indicated in the legends are carried out by using the Chaboche model. The Chaboche and the Tanimura model are both overstress models and therefore they lead under the assumption of perfect plasticity to nearly identical results. However, different material parameter procedures were applied to these models. The Bodner–Partom model does not distinguish between elastic and plastic material properties, therefore, the material parameter identification procedure of the Bodner–Partom law differs from that of overstress models. This could be a reason for the differences between the presented simulations.

6. Conclusions

The presented experimental set-up turned out to be appropriate for measuring plate deflections and loading histories during the impulse duration. It was possible to record the dynamic response of metal

plates in order to obtain realistic load displacement dependencies which were compared to simulated results. In the simulations special attention was focused on the propagation of bending moments and it was shown that they have been most responsible for the spread of plastic zones in the plate. Immediately after the shock wave has loaded the plate the plastification depended on the oscillation of the bending moment in superposition with the normal force. For that reason simplifications were only as long possible as the propagating bending moments could still be predicted realistically. Therefore it was necessary to include the elastic material properties in the simulations.

Using the Chaboche model elastic, hardening and viscous material properties can be separated from each other. This allows in the material parameter identification procedure a precise adaption of the viscoplastic law to the uni-axial tension tests. In the Bodner–Partom model elastic properties are not assumed and hardening as well as viscous behaviors are combined with each other. In the Tanimura model the hardening is neglected. With this described advantage in the case of the elastic–viscoplastic Chaboche model simulations using this law lead to the most precise results.

Acknowledgements

The author would like to thank Prof. Dr. Dieter Weichert and Prof. Dr. Rüdiger Schmidt from Institute of General Mechanics, RWTH Aachen, Germany for their kind support and helpful discussions.

References

Andrade, E.N., Da, C., 1910. On the viscous flow of metals and allied phenomena. Proc. Roy. Soc. (A), London 85, A567.

Batra, R.C., Jaber, N.A., Malsbury, M.E., 2003. Analysis of failure modes in an impact loaded thermoviscoplastic prenotched plate. Int. J. Plast. 19, 139–196.

Bodner, S.R., Partom, Y., 1975. Constitutive equations for elasto-viscoplastic strain-hardening materials. ASME J. Appl. Mech. 42, 385–389.

Bruhns, O.T., 1987. Einige Bemerkungen zur Beschreibung inelastischer Prozesse im Bereich hoher Deformationsgeschwindigkeiten. ZAMM 67, T181–T183.

Chaboche, J.L., 1989. Constitutive equations for cyclic plasticity and cyclic viscoplasticity. Int. J. Plast. 5, 247–302.

Chan, K.S., Bodner, S.R., Lindholm, U.S., 1988. Phenomenological modelling of hardening and thermal recovery in metals. J. Eng. Mat. Tech. 110, 1–8.

Colak, O.U., 2004. A viscoplasticity theory applied to proportional and non-proportional cyclic loading at small strains. Int. J. Plast. 20, 1387–1401.

Cristescu, N., 1967. Dynamic Plasticity. North-Holland, Amsterdam.

Doyle, J.F., 1997. Wave Propagation in Structures. Springer-Verlag.

Eftis, J., Carrasco, C., Osegueda, R.A., 2003. A constitutive-microdamage model to simulate hypervelocity projectile-target impact, material damage and fracture. Int. J. Plast., 1321–1354.

Florence, A.L., 1966. Circular plate under a uniformly distributed impulse. Int. J. Sol. Struct. 2, 37–47.

Gerard, G., 1956. A new experimental technique for applying impulse loads. In: Proc. Symp. on Impact Testing, Atlantic City.

Gurtin, M.E., 2003. On a framework for small-deformation viscoplasticity: free energy, microforces, strain gradients. Int. J. Plast. 19, 47–90.

Haupt, P., Kersten, Th., 2003. On the modelling of anisotropic material behaviour in viscoplasticity. Int. J. Plast. 19, 1885–1915.

Häusler, O., Schick, D., Tsakmakis, Ch., 2004. Description of plastic anisotropy effects at large deformations. Part II: The case of transverse isotropy. Int. J. Plast. 20, 199–223.

Imatani, S., Kokubo, K., Inoue, T., 1991. Rate dependent stress/strain response of a notched cylinder. In: Jono, M., Inoue, T. (Eds.), Proceedings of the Sixth International Conference on Mechanical Behaviour of Materials, 20.7.–2.8.1991, p. 793.

Idczak, W., Rymarz, Cz., Spychała, A., 1981. Studies on shock-wave loaded, clamped circular plates. J. Tech. Phys. 22, 175–184.

Iyer, S.K., Lissenden, C.J., 2003. Multiaxial constitutive model accounting for the strength-differential in Inconel 718. Int. J. Plast. 19, 2055–2081.

Jones, N., 1989. Structural Impact. Cambridge University Press.

Kajberg, J., Sundin, K.G., Melin, L.G., Stahle, P., 2004. High strain-rate tensile testing and viscoplastic parameter identification using microscopic high-speed photography. Int. J. Plast. 20, 561–575.

Kalthoff, J.F., 2000. Modes of dynamic shear failure in solids. Int. J. Fract. 101, 1–31.

Kalthoff, J.F., Winkler, S., 1987. Failure mode transition at high rates of shear loading. In: Chiem, C.Y., Kunze, H.D., Meyer, L.W. (Eds.), Impact Loading and Dynamic Behavior of Materials, vol. I, pp. 185–195.

Kłosowski, P., Woznica, K., Weichert, D., 1995. A comparative study of vibrations of elasto-viscoplastic shells and plates. Engng. Trans. 43, 183–204.

Kreja, I., Schmidt, R., Reddy, J.N., 1997. Finite elements based on a first-order shear deformation moderate rotation shell theory with applications to the analysis of composite structures. Int. J. Non-Linear Mech. 32, 1123–1142.

Krempl, E., Khan, F., 2003. Rate (time)-dependent deformation behavior: an overview of some properties of metals and solid polymers. Int. J. Plast., 1069–1095.

Krempl, E., McMahon, J.J., Yao, D., 1984. Viscoplasticity based on overstress with a differential growth law for equilibrium stress. In: Mechanics of Materials, 2nd Symp. on Non-linear Constitutive Relations for High temperature Applications, NASA, Cleveland, OH, vol. 5, p. 35.

Lehmann, T., 1984. General frame for definition of constitutive laws for large nonisothermic elastic–plastic and elastic–viscoplastic deformations. In: The Constitutive Law in Thermoplasticity CIMS Cours and Lectures, vol. 281. Springer-Verlag, Wien, New York.

Lemaitre, J., Chaboche, J.L., 1994. Mechanics of Solid Materials. Cambridge University Press.

Lin, R., Brocks, W., 2004. On a finite strain viscoplastic theory based on a new internal dissipation inequality. Int. J. Plast. 20, 1281–1311.

Lubarda, V.A., Benson, D.J., Meyers, M.A., 2003. Strain-rate effects in rheological models of inelastic response. Int. J. Plast. 19, 1097–1118.

Malvern, L.E., 1951. Plastic wave propagation in a bar of material exhibiting a strain rate effect. Quart. Appl. Math. 8, 405–411.

Norton, F.N., 1929. Creep of High Temperatures. McGraw-Hill Book Company, New York.

Palmerio, A.F., Reddy, J.N., Schmidt, R., 1990. On a moderate rotation theory of laminated anisotropic shells, Part 1—Theory, Part 2—Finite element analysis. Int. J. Non-Linear Mech. 25, 687–714.

Perzyna, P., 1963. The constitutive equations for rate sensitive plastic materials. Quart. Appl. Math. 20, 321–332.

Renard, J., Pennetier, O., 1996. Nonlinear dynamic response of plates submitted to an explosion, numerical and experimental study. In: Structural Dynamics-EURODYN'96, Balkema, Rotterdam, p. 689.

Rizzi, E., Hähner, P., 2004. On the Portevin–Le Chatelier effect. Int. J. Plast. 20, 121–165.

Schmidt, R., Reddy, J.N., 1988. A refined small strain moderate rotation theory of elastic anisotropic shells. ASME J. Appl. Mech. 55, 611–617.

Schmidt, R., Weichert, D., 1989. A refined theory of elastic–plastic shells at moderate rotations. ZAMM 69, 11–21.

Schneidler, M., Wright, T.W., 2003. Classes of flow rules for finite viscoplasticity. Int. J. Plast. 19, 1119–1165.

Stoffel, M., 2000. Nichtlineare Dynamik von Platten. Ph.D. Thesis, RWTH, Aachen.

Stoffel, M., Schmidt, R., Weichert, D., 1998. Vibrations of viscoplastic plates under impact load. In: Jones, N., Talaslidis, D.G., Brebbia, C.A., Manolis, G.D. (Eds.), Structures under Shock and Impact, vol. 5. Computational Mechanics Publications, Southampton-Boston, pp. 299–308.

Stoffel, M., Schmidt, R., Weichert, D., 2001a. Experiment und Simulation stoßwellenbeanspruchter Platten. ZAMM 81, S231–S232.

Stoffel, M., Schmidt, R., Weichert, D., 2001b. Shock wave-loaded plates. Int. J. Solids Struct. 38, 7659–7680.

Stronge, W.J., Yu, T.X., 1993. Dynamic Models for Structural Plasticity. Springer-Verlag.

Tanimura, S., 1979. A practical constitutive equation covering a wide range of strain rates. Int. J. Eng. Sci. 17, 997–1004.

Taylor, G.I., 1940. Propagation of earth waves from an explosion. In: British Official Report R.C. Vol. 70.

Tsakmakis, Ch., 2004. Description of plastic anisotropy effects at large deformations. Part I: Restrictions imposed by the second law and the postulate of Il'iushin. Int. J. Plast. 20, 167–198.

Uenishi, A., Teodosiu, C., 2004. Constitutive modelling of the high strain rate behaviour of interstitial-free steel. Int. J. Plast. 20, 915–936.

von Kármán, T., 1942. On the propagation of plastic deformation in solids. In: N.D.R.C. Report, Nr. A-29 (O.S.R.D. Nr. 365).

Voyiadjis, G.Z., Al-Rub, R.K.A., Palazotto, A.N., 2004. Thermodynamic frame work for coupling of non-local viscoplasticity and non-local anisotropic viscodamage for dynamic loacalization problems using gradient theory. Int. J. Plast. 20, 981–1038.

Walker, K.P., 1981. Research and development program for non-linear structural modeling with advanced time-temperature dependent constitutive relationships. In: Report PWA-5700-50, NASA CR-165533.

Weichert, D., Stoffel, M., 1998. Theoretical and experimental investigations on plates under impulsive loading. In: Theocaris, P.S., Fotiadis, D.I., Massalas, C.V. (Eds.), Proc. 5th National Congress on Mechanics, vol. 1. University of Ioannina Press, Ioannina, pp. 72–83.

Wierzbicki, T., Florence, A.L., 1970. A theoretical and experimental investigation of impulsively loaded clamped circular viscoplastic plates. Int. J. Sol. Struc. 6, 553–568.